Available online at www.sciencedirect.com
ScienceDirect
C. R. Physique 10 (2009) 528–536
COMPTES RENDUS PHYSIQUE

Theoretical spectroscopy / Spectroscopie théorique

Ionic displacement caused by electronic excitations

Michael Rohlfing

Fachbereich Physik, Universität Osnabrück, Barbarastraße 7, 49069 Osnabrück, Germany

Available online 15 August 2009

Abstract

Electronic excitations are often accompanied by displacement of the ions from their ground-state equilibrium positions. This leads to line broadening of optical spectra, Stokes shifts, conformational changes, and photoinduced reactions. Here we discuss approaches to these features within ab-initio methods, in particular within many-body perturbation theory. A number of various systems, including molecules, point defects, polymers, and surfaces, are discussed to illustrate issues like localization and self-trapping that are relevant for a detailed understanding of the interrelation between excited states and geometrical structure. ***To cite this article: M. Rohlfing, C. R. Physique 10 (2009).***

Résumé

Déplacement des ions provoqué par des excitations électroniques. Les excitations électroniques s'accompagnent souvent par un déplacement des ions de leur position d'équilibre dans l'état fondamental. Ceci induit un élargissement des raies des spectres optiques, des Stokes shifts, des changements de conformation, et des réactions photo induites. Dans cet article nous discutons des approches pour traiter ces effets avec des méthodes ab initio, en particulier dans le cadre de la théorie des perturbations à plusieurs corps. Nous discutons différents systèmes dont des molécules, des défauts ponctuels, des polymères, et des surfaces, afin d'illustrer des problématiques tels que la localisation et l'auto-piégeage qui sont importants pour comprendre la relation entre états excités et structure géométrique. ***Pour citer cet article : M. Rohlfing, C. R. Physique 10 (2009).***

Keywords: Ab-initio electronic structure; Excited state; Optical spectrum

Mots-clés : Structures électroniques ab initio ; État excité ; Spectre optique

1. Introduction

The last two decades have seen enormous progress in the theoretical description of electronic and optical excitation of condensed matter [1]. Important achievements in this field are due to the development of (static and time-dependent) density-functional theory (DFT, TDDFT) and ab-initio many-body perturbation theory (MBPT). It has become possible to calculate electronic and optical excitations with unprecedented accuracy, providing excitation energies and the corresponding wave functions, from which the spectra can be evaluated.

Most of the discussion of spectra so far has been based on the concept of a fixed geometry, i.e. a geometry which is simply defined by the mechanical equilibrium of the electronic ground state. In this context one mainly analyses

E-mail address: Michael.Rohlfing@uos.de.

1631-0705/$ – see front matter
doi:10.1016/j.crhy.2009.07.001

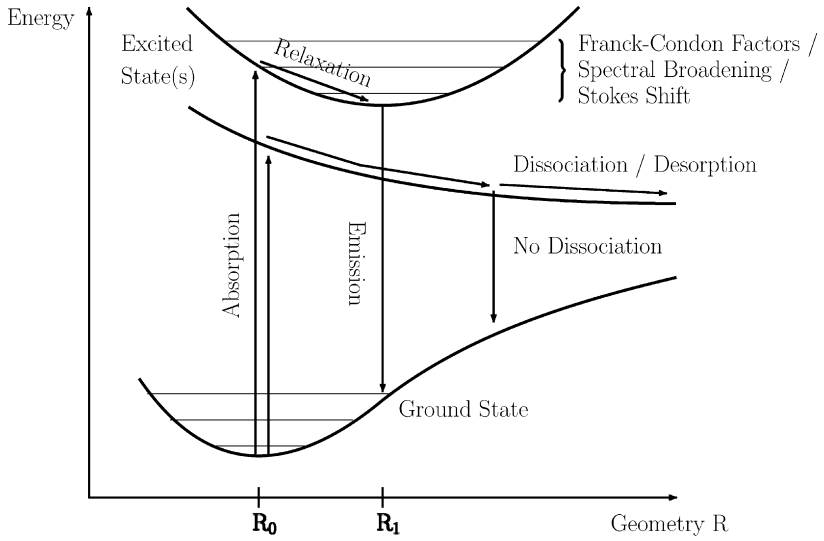

Fig. 1. Schematic illustration of the ground state and excited state(s) of a condensed-matter system as depending on a generalized coordinate(s) (here: one-dimensional).

vertical transitions between the ground state and excited state(s) of the electronic structure. Such considerations allow to investigate the energetic position and spectral weight of typical lines in the spectrum (more precisely, the average energy and the total optical weight of spectral peaks), which is often sufficient to characterize systems (crystals, molecules, polymers, surfaces, defects, and more). Many details of the spectra, however, are simply disregarded by limiting the discussion to vertical transitions, only. Features like spectral broadening, Stokes shifts, and excited-state induced ionic dynamics (leading to dissociation, desorption, etc.) are not described when the geometry is kept frozen [2].

All features mentioned above result from the fundamental observation that in many systems the mechanical equilibrium of the excited state is different from that of the ground state. This statement holds in particular for strongly localized excited states. Such states induce significant wave-function amplitude and effective charge changes at the involved atoms, thus causing significant forces on and displacement of the ions. The purpose of the present article is to show how ab-initio excited-state approaches can be combined with the concept of geometrical displacement.

Effects of geometrical displacement have long been investigated by quantum-chemical approaches [3]. Such methods may, however, not be suitable for extended systems, which rather require techniques based on DFT and/or MBPT. Nonetheless, many of the findings of quantum chemistry can be transferred to extended systems, as well. Furthermore, plenty of discussion has been taken place on the basis of empirical models. One of the most important tasks is therefore the transfer of the knowledge from models and from quantum chemistry into the context of other ab-initio electronic-structure methods.

Fig. 1 illustrates several features relevant in the context of excited-state related ionic movement. The electronic ground state has a total-energy minimum at equilibrium configuration $\mathbf{R}_0$. Excitation by light absorption puts the system into one of its excited states, which will usually have its total-energy minimum at a different geometry (if it has a minimum in the first place). As a result, several effects may occur:

(i) If the excited state does have a total-energy minimum, the quantization of the ionic motion will yield vibronic sublevels (this is also true for the ground state). Excitation thus occurs from the lowest ground-state sublevel (in which the system resides if the temperature is low enough) into one of the excited-state sublevels, i.e. the spectrum splits into a lowest-energy "zero-phonon transition" (i.e. excitation into the lowest excited-state sublevel) and further lines at higher energy, with the splitting between the peaks given by the excited-state vibrational frequency. The intensity of each peak would be given by the overlap of the ionic wave functions of the vibrational sublevels of the ground and excited electronic state (i.e. by the Franck–Condon factors). Maximum amplitude is obtained for those transitions that are close to the vertical transition energy at $\mathbf{R}_0$, i.e. the "classical" transition

energy (indicated in Fig. 1 as vertical arrow), and the difference between the energy of maximum absorption intensity and the low-energy onset of the absorption spectrum roughly corresponds to the relaxation energy in the excited state between $\mathbf{R}_0$ and $\mathbf{R}_1$. One should note that in many cases the vibrational sublevels are broadened further and may not be resolved; in such cases one can still evaluate the overall line shape resulting from the Franck–Condon factors and compare with the experimental spectrum. As a rough estimate in many cases, the excited-state relaxation energy gain approximately corresponds to the width of the absorption peak.

(ii) Similar to the vibrational side bands or broadening of the absorption peak, the reverse transition (which occurs long after the system has relaxed to the vibrational ground state of the excited electronic state) from the excited state back to the ground state is subject to the same effects. Here the emission spectrum will show side bands and broadening, as well. Maximum intensity occurs again near the "classical" transition energy (indicated in Fig. 1 as vertical arrow), while maximum transition energy is given by the "zero-phonon transition" between the vibrational ground states of the ground and excited electronic state. Note that the zero-phonon transition is the same in absorption and emission. Finally, the Stokes shift (i.e. the difference between the absorption and emission peak energies) roughly equals the sum of the two relaxation energies between $\mathbf{R}_0$ and $\mathbf{R}_1$ (i.e., in the ground and excited electronic state).

(iii) If the excited state does not have a total-energy minimum, the picture as described above does not hold. The structure of the absorption spectrum will again exhibit broadening due to the quantum nature of the ionic motion in the excited state. The ionic motion, however, is more complicated than discussed above. Most importantly, the system will undergo dynamics that might lead to complete dissociation into two components (i.e. photodissociation of a molecule, photodesorption of a molecule from a surface, etc.). Different from phenomena (i) and (ii), this can already be understood to some degree by assuming classical motion of the system, and may be discussed by employing conventional molecular-dynamics techniques (applied to the excited electronic state). Such "adiabatic dynamics" may allow to investigate dissociation trajectories, ionic kinetic energies, and time scales of the processes.

(iv) Although conventional molecular dynamics ("adiabatic dynamics") might appear sufficient for investigating dissociation, many systems do exhibit non-adiabatic effects, i.e. interrelation between the electronic levels beyond the Born–Oppenheimer approximation. As the geometry of the system changes, the electronic states evolve and may get admixtures from other states. In such cases, the system may hop from one electronic state onto another during ionic dynamics, in particular when the energy difference between two electronic levels becomes small (as is the case for avoided crossing, conical intersections, etc.). In particular, the system may jump from one excited state to another, or it might jump from the excited state back to the ground state, which may stop or reverse the dissociation process. Note that such effects are of quantum nature, i.e. they do not occur in a deterministic way but require probability considerations based on ionic wave functions and wave packets. Consequently, the final dissociation probability may be smaller than 1 ("quenching"), in some cases by several orders of magnitude.

Based on these general considerations, several challenges have to be faced in the context of electronic-structure theory: (i) the precise determination of geometry-dependent total energies and excitation energies; (ii) the determination of the corresponding forces; (iii) total-energy minimization to determine equilibria, displacements, Franck–Condon factors, spectral broadening, and Stokes shifts; (iv) conventional adiabatic molecular dynamics to discuss "classical" dissociation paths, kinetic energies, etc. (in one or more dimensions); and (v) non-adiabatic quantum dynamics of the ions in the potential energy surfaces provided by (i)–(iii). One may add another issue: (vi) the lifetime of an excited electronic states may be finite due to Coulomb scattering or charge-transfer processes, which may change the ionic dynamics since the system might change its electronic state independent of ionic-motion features;. Last but not least, (vii) electronic dynamics and ionic dynamics might even be coupled.

2. Excited-state total energies and forces

Provided that the excited state $|S\rangle$ is an individual state well separated in energy from any other states, one can safely assume that the Born–Oppenheimer approximation (which is commonly assumed for the ground state) will hold for the excited state, as well. In that case, it is trivial to define its total energy (including the dependence on geometry) as

$$E_{tot}^{S}(\mathbf{R}) = E_{tot}^{gs}(\mathbf{R}) + \Omega_S(\mathbf{R}) \tag{1}$$

with $E_{tot}^{gs}(\mathbf{R})$ being the total energy of the system in its electronic ground state and $\Omega_S(\mathbf{R})$ the excitation energy, as a function of all nuclear coordinates $\mathbf{R}$. Here we mention three common ab-initio approaches to calculate $\Omega_S(\mathbf{R})$ (or directly $E_{tot}^{S}(\mathbf{R})$) for a given configuration $\mathbf{R}$: constrained DFT [4], time-dependent DFT (TDDFT), and many-body perturbation theory (MBPT) which consists of the GW method for single-particle excitations plus the Bethe–Salpeter equation (BSE) for optical excitations [1]. Within constrained DFT (CDFT), one assumes that the electronic structure of the excited state is simply given by the de-occupation of one hole state and the occupation of one electron state. This can simply be realized within a standard DFT approach, and can even distinguish between different spin configurations (e.g., singlet-to-singlet vs. singlet-to-triplet transitions) provided that spin-polarized DFT is employed. CDFT directly yields the total energy of the constrained state, $E_{tot}^{S}(\mathbf{R})$, and the related ionic forces, $-\partial_{\mathbf{R}} E_{tot}^{S}$, without decomposition into ground-state and excitation contribution. Such a CDFT treatment can be physically meaningful if the excited state is mainly given by a transition between one hole state and one electron state (without significant band dispersion), which would be the case for some deep point defects or the HOMO-LUMO transition in some molecules. In most cases, however, an excited state involves electron–hole correlation both among hole or electron bands and in real and reciprocal space, which means that the state in question cannot be represented by a simple band-to-band transition such as in CDFT. Surprisingly, even for such cases, CDFT may yield reasonable results for excited-state forces [4,5].

Within TDDFT and MBPT, electron–hole correlation among various hole and electron bands and in real/reciprocal space is considered (regardless of the question to which extent the available kernels of TDDFT do describe excitons in extended systems) and can yield a realistic description of the excited state and the involved excitation energy, $\Omega_S(\mathbf{R})$. From Eq. (1), the force $-\partial_{\mathbf{R}} E_{tot}^{S}$ is composed of two contributions, i.e. $-\partial_{\mathbf{R}} E_{tot}^{S} = -\partial_{\mathbf{R}} E_{tot}^{gs} - \partial_{\mathbf{R}} \Omega_S$. The force from the ground state, $-\partial_{\mathbf{R}} E_{tot}^{gs}$, is immediately given by any modern DFT computer code (provided that DFT is sufficient for describing the ground state). The calculation of the excitation contribution, $-\partial_{\mathbf{R}} \Omega_S$, is more difficult since both TDDFT and MBPT involve a more complicated two-particle Hamiltonian from which $\Omega_S(\mathbf{R})$ results, and its derivative is more difficult to evaluate. As discussed by Ismail-Beigi and Louie [6], it can be obtained within MBPT be applying the Hellman–Feynman theorem, i.e.

$$\partial_{\mathbf{R}} \Omega_S = \langle S | (\partial_{\mathbf{R}} \hat{H}) | S \rangle \tag{2}$$

which is also valid within TDDFT. The analytic derivative $\partial_{\mathbf{R}} \hat{H}$ of the two-particle Hamiltonian $\hat{H}$ (which contains the single-particle physics of the electron and of the hole, as well as the electron–hole interaction) is a complicated issue, but might be simplified according to suggestions discussed in Ref. [6]. In any case, Eq. (2) provides an analytic expression of all force components, to be evaluated on the basis of just one MBPT calculation at configuration $\mathbf{R}$.

Alternatively, forces and dynamics can be addressed by defining a low-dimensional subspace of the configuration space (i.e. one or a few dominant normal coordinates along which displacement will be of relevance) and by carrying out MBPT or TDDFT calculations on a grid. This seems more demanding at first glance and might even be considered as an unnecessary restriction. However, such a procedure is necessary if one wants to investigate ionic quantum dynamics beyond the Born–Oppenheimer approximation, involving detailed knowledge about energies and wave functions of more than one state and for more than just one geometrical configuration.

In all cases discussed below we employ DFT + MBPT (i.e. GW approach plus the Bethe–Salpeter equation, BSE) for a restricted, mostly one-dimensional generalized coordinate which characterizes the displacement. In those cases where this one-dimensional coordinate X refers to displacement of many atoms (in particular, CaF_2, PPP, and Si(111)-(2×1)) the displacement pattern was obtained from CDFT (or even a simple tight-binding scheme for Si(111)-(2×1)). The excitation energies $\Omega_S(X)$ were then calculated within MBPT for selected values of the generalized coordinate X.

It should be noted that MBPT at its current status, although being our method of choice, does not yield the same level of accuracy as wave-function based quantum-chemistry approaches [3] or quantum-Monte-Carlo techniques [7] can achieve if driven to convergence. One reason is that quantum-chemical methods like configuration–interaction or coupled-cluster approaches employ the exact Hamilton operator of the system and can systematically explore the full many-body Hilbert space, including exchange and correlation effects in an exact way. These methods can thus provide an answer as close to the exact result as desired (although at extremely high cost and associated with very unfavorable scaling with system size). MBPT, on the other hand, uses an approximate (but, of course, very well motivated and sophisticated) Hamilton operator (i.e., self-energy operator Σ) to describe correlation. The systematic inclusion of higher terms beyond $\Sigma = iGW$ is possible, in principle, but nearly never realized. Furthermore, additional (however, well-established) approximations are employed, like the use of static screening for the electron–hole interaction, the

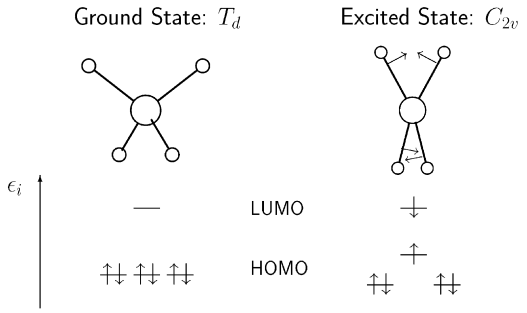

Fig. 2. Geometry of the methane molecule (CH_4) in its electronic ground state (left) and excited state (right).

quasiparticle approximation for the frequency-dependent structure of the Green functions, etc. As a result of all these issues, MBPT data are accurate to within about 0.1 eV at best.

As an example, the most accurate approaches (coupled-cluster, complete-active-state-self-consistent-field, and quantum-Monte-Carlo techniques [7]) yield a vertical singlet (triplet) excitation energy of methane of 9.1 eV (8.7 eV), while MBPT yields 9.2 eV (8.5 eV), thus deviating by 0.1–0.2 eV. The real power of MBPT is in its general form, which does equally well apply to systems of various size, dimension, and chemical composition, thus allowing for a systematic comparison between different systems, like a comparison between a free molecule and one adsorbed on a surface, a comparison between surface and bulk excitations, etc. Such investigations would be extremely difficult for quantum-chemical approaches.

3. Stokes shift and spectral broadening

The most common effects of the spatial shift between ground-state and excited-state equilibria are given by spectral broadening and Stokes shifts of the optical transition between ground and excited states (see the discussion of Fig. 1). Here we discuss a number of examples which have been investigated in terms of the methods explained above. As characteristic quantities we show the vertical transition energy, the relaxation gain in the excited state, the spatial range of the excitation, and the maximum displacement of atoms (at or near the center of the excitation). The systems and states are sorted by dimension, from an isolated molecule and a zero-dimensional point-defect system to a one-dimensional polymer and a two-dimensional semiconductor surface. This dimensionality, together with the spatial extent of the excitation, are directly related to the relaxation energy to be gained in the excited state.

The localization and the spatial extent of the excitation is one of the key quantities in this context. Depending on the nature of the system, localization can occur in two ways:

(i) Localization results immediately if the system has localized single-particle levels for both the electron and the hole, or if one particle is from a localized single-particle level and the other particle attracted to it by electron–hole interaction. One example for this situation is given by the CH_4 molecule in which localization of the hole is caused by quantum confinement of the entire molecule [7]. The associated re-organization of particles and their charges leads to forces on the nuclei and corresponding displacement, as illustrated in Fig. 2 which shows the distortion of the CH_4 molecule in its excited state. As indicated below each panel, the ground-state configuration has a three-fold degenerate HOMO level (resulting from the tetrahedral T_d symmetry of the molecule). The excitation breaks this degeneracy and consequently lowers the symmetry to C_{2v} (Jahn–Teller distortion). The associated atomic displacement and relaxation energy is quite large (see Table 1).
A similar situation is given by the F center of CaF_2 [8,5] which hosts a localized hole state but no localized electron state. In all such cases the spatial size of the electron–hole excitation is closely related to the size of the localized single-particle state(s), or it might even be smaller (due to electron–hole attraction). In the case of the F center of CaF_2 a deep hole state causes hole localization of about 4 Å leading to attraction of the electron to the hole and thus to the formation of an exciton of roughly the same size. Note that without attraction to the hole, the defect electron states would be in resonance with the CaF_2 conduction and would thus be of delocalized nature.
Note that in most molecules (including the case of CH_4 discussed above) the electron state on its own would not be bound strongly (i.e. the electron affinity would be very small). Similarly, the F center of CaF_2 does not show

Table 1
Excited-state relaxation data of singlet-to-singlet excitations in various systems, as calculated within DFT + MBPT.

System	Ω [eV]	ΔE_{tot} [eV]	Size [Å]	max. ΔX [Å]
CH_4 molecule [7]	10.5	1.9	2	0.3
CaF_2 F center [5]	3.4	0.8	4	0.14
PPP polymer [4]	3.6	0.22	20	0.4
Si(111)-(2 × 1) surf. exciton [17]	0.45	0.035	60	0.035

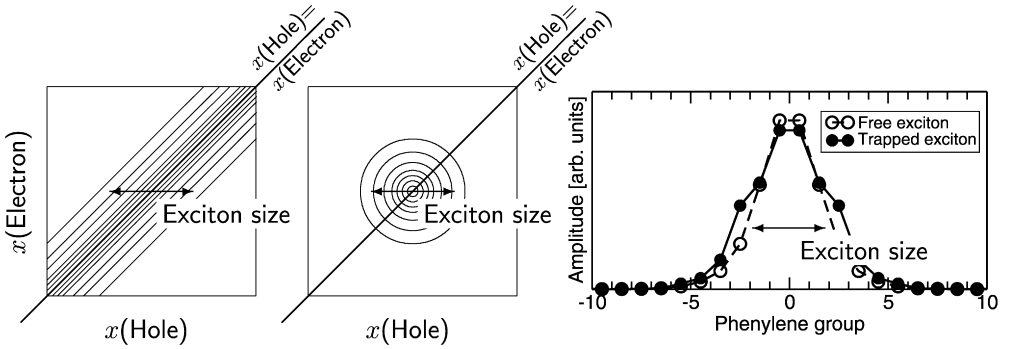

Fig. 3. Left and middle panels: Schematic illustration of the two-particle wave function of a free exciton (left) and a bound exciton (middle; binding either by defects or by self-trapping). Right panel: corresponding data for the one-dimensional semiconductor poly-para-phenylene (PPP).

localized electron states, either. In both cases an excited electron on its own (e.g. in inverse photoemission experiments) would be delocalized and might not cause significant forces and displacement (actually, the corresponding issues of polaron formation are of quite different nature). In the present context, however, hole and electron are created simultaneously in terms of a Coulomb-bound pair, which is bound to the molecule or defect because the hole is bound to it and the electron has to follow.

(ii) The situation is more difficult if the system does not have an explicitly localized single-particle state. In such a case localization can nonetheless occur due to a self-trapping mechanism [9]. This requires that the gap energy between electron and hole states decreases (which gains energy for the electron–hole excitation) when the atoms are displaced (which costs elastic energy in the ground state). Since the gain in gap energy depends linearly on atom displacement while the cost in elastic energy depends quadratically, a net gain of energy is achieved. This gain in energy constitutes an effective interaction potential between the atoms and the exciton. This, however, can only happen when finite displacement is achieved. An exciton which is macroscopically delocalized causes infinitesimally small force on each atom, and thus no displacement. Note that such a combination of exciton and atomic distortion is still mobile as a whole, i.e. a simultaneous shift of both the distortion pattern and the electron–hole excitation is possible. The self-trapped exciton might thus also be considered as an "excitonic polaron".

The spatial size of a self-trapped exciton must not be confused with the internal electron–hole correlation length of a non-trapped (free) exciton. The latter results from the attraction between electron and hole while the former refers to the spatial extent of both the hole and the electron (and thus the exciton) for a trapped state. The difference is illustrated schematically in Fig. 3 which shows the two-particle wave function of a free exciton (left panel) and of a trapped exciton (middle panel) for a one-dimensional system. Both kinds of exciton size are different from each other, in principle. In practice, however, we have found in many systems that the trapping size roughly equals the electron–hole correlation length inside the free exciton, which allows to estimate real-space trapping from the properties of the free exciton. As illustration, the right panel of Fig. 3 shows the size of the free and of the trapped exciton in poly-para-phenylene (PPP; cf. Table 1) [4]. Both the intrinsic electron–hole distance inside the free exciton and the localization range of the self-trapped exciton amount to about 5 phenylene rings, i.e. about 20 Å [4].

In this polymer, being a chain system in vacuum, the electron and the hole are immediately confined in the directions perpendicular to the polymer chain. Along the chain, the remaining quantum mechanics is quasi-one-dimensional, which explains the significant energetic effects (large electron–hole interaction, strong trapping, large

Stokes shift) observed for the material [10,11]. Note that the probability distribution for the electron or hole of the trapped exciton immediately yields a local charge transfer, to which the force on and (due to Hooke's law) the displacement of the nuclei is proportional. Therefore the probability distribution of the hole and/or electron and the resulting atom displacement pattern are basically the same. In PPP the main effect of the electronic excitation is to change the C–C bonds between the phenylene rings from single-bond nature (associated with the valence band) to double-bond nature (associated with the conduction band), thus forcing the material into a flattened configuration which it would no accept in its electronic ground state [4]. The corresponding lowering of the fundamental gap, which constitutes an attractive potential for the exciton, is the driving force which localizes the exciton at the position of the geometric distortion (i.e., self-traps the exciton).

In conventional semiconductors effects like self-trapping hardly occur, for the reason just discussed: the size of the exciton is quite large (covering $\sim$1000 atoms), and thus its amplitude at and force on each atom are too small to cause significant displacement. This situation changes in the case of the Si(111)-(2×1) surface [12–17] which (due to the existence of dangling-bond surface bands for both the hole and the electron) provides localization of both particles at the surface (localization of type (i), see last paragraph). Furthermore, due to very weak band dispersion perpendicular to the surface Pandey chains similar localization of type (i) occurs across the chains, as well (although not as strong as perpendicular to the surface). The resulting exciton is thus a quasi-one-dimensional object with an electron–hole correlation length of about 40 Å (corresponding to about 20 surface atoms). Therefore the self-trapping of this state (i.e. additional localization of type (ii) along the Pandey chain) causes enough amplitude on the atoms involved (up to about 10% in the center of the exciton). Since the excited electron and hole reside at different atoms (the hole at the up atom, the electron at the down atom of the Pandey chain), enough charge transfer occurs to cause significant force (and thus displacement) on the atoms. The displacement of the atoms, in turn, lowers the band gap locally, which lowers the excitation energy of the exciton and thus stabilizes the trapping. In total, self trapping lowers the total energy by about 35 meV [17].

Since the electron–hole interaction is weaker than in PPP (due to dielectric screening in the substrate), and because of stronger band dispersion along the chain, the size of the exciton is significantly larger than in PPP and the energetic effects due to self-trapping are one order of magnitude weaker.

The strength of the displacement of the individual atoms is related to the size of exciton, as well. The displacement of an atom depends on the force on the atom, which (from simple electrostatics) is proportional to the charge density of the excited electron and hole near the atom. This charge density is inverse proportional to the number of atoms involved in the displacement pattern, which in turn is proportional to the size of the excited state. Simply speaking, the more atoms are involved in the excitation, the smaller the displacement of every atom will be. In three-dimensional semiconductors the exciton can have a range of several nanometers, thus covering thousands of atoms, yielding very small charge-density change at each atom and thus negligible displacement, relaxation energy gain, broadening, and Stokes shift. Deformation-related broadening and Stokes shifts usually result for strongly localized excited states, low-dimensional systems, or defects.

The displacement of an atom is not only controlled by the force on it, but also by the stiffness of the material along the force. Exceptionally large displacements are observed when conformational changes are induced by the excitation. One example is given by PPP, which consists of phenylene rings twisted relative to one another. Upon excitation the phenylene rings rotate relative to each other (with the rotational axis given by a carbon–carbon single bond, which easily allows for rotation). Since the material is relatively soft with respect to this rotation, the displacements in PPP are quite large — even larger than those in the CH_4 molecule where the excitation is localized on just five atoms.

4. Dissociation dynamics

If the excited-state potential-energy surface has no minimum, the system may dissociate in two parts. Typical examples are the photo-induced desorption of molecules from surfaces and the photodissociation of molecules and other systems. One well-studied class of systems is given by alkali-halide surfaces, like the potassium iodide (001) surface [18–21]. Such dynamics may even be described by classical molecular dynamics, which is conceptually simpler than the quantum-dynamics effects discussed above.

As illustration, Fig. 4 shows the expulsion of an iodine atom from the KI(001) surface as a result of laser excitation of the surface exciton. In a simplified picture the atom in question is expelled vertically and all other atoms remain in

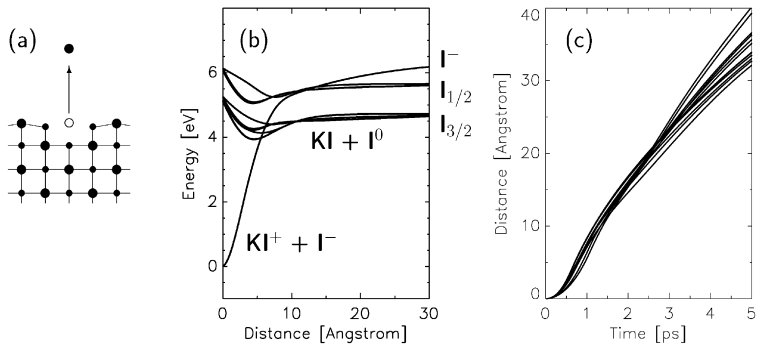

Fig. 4. Expulsion dynamics of a neutral iodine atom from the KI(001) surface. Left panel: Geometric structure, showing the vertical expulsion of the iodine atom along a one-dimensional line. Middle panel: Total energy of the ground state and of 12 excited states as a function of the vertical position of the expelled iodine atom. Right panel: resulting one-dimensional trajectory of the expulsion process, corresponding to the excited-state potential energy shown in the middle panel.

their ground-state position. Therefore the entire energetics and dynamics can be described by just one coordinate, i.e. the height of the iodine atom above the surface.

The expulsion is triggered by a laser pulse, which creates an exciton. Experiment indicates that the excitation occurs directly in terms of a surface exciton rather than via a bulk exciton traveling to the surface. The surface exciton is characterized by an electron which extends a little into the vacuum, accompanied by a hole at the iodine surface atom [22]. Note that the hole might be given by any of the three p valence orbitals of the iodine anion, and might form a spin-singlet or spin-triplet configuration with the electron, which (due to spin–orbit interaction at the iodine atom) reorganizes into $j = 1/2$ and $j = 3/2$ excitons, i.e. there are 12 possible surface excitons. The angular momentum of the exciton finally shows up as the angular momentum of the expelled iodine atom.

The spatial difference of the electron and hole and of the corresponding charge densities causes a net force on the iodine atom results which drives the atom out of the surface (cf. middle panel of Fig. 4). After a distance of about 10 Å the excited-state potential energy levels out (corresponding to a charge-neutral substrate and charge-neutral iodine atom) while the ground-state potential energy (starting at 0 eV for $z = 0$ Å) exhibits strong Coulomb attraction between the negatively charged I^- anion and a positively charged substrate. While the details at and beyond 10 Å are of minor importance, the steep initial drop of all excited-state curves between 0 and 5 Å causes fast acceleration of the iodine atom to a velocity of about 1000 m/s within about one picosecond, followed by slight de-acceleration afterwards. In all cases the iodine atom leaves the surface as a neutral atom at a velocity of several 100 m/s, corresponding to a kinetic energy of several 100 meV. This picture is confirmed by experiments which combine pulsed laser excitation with time-of-flight detection of the expelled halogen atoms [19].

Such classical dynamics considerations disregard several important features [21]. First, the one-dimensional consideration is certainly oversimplified. Elementary considerations of conservation of momentum yield that the substrate must pick up the recoil of the expelled iodine atom, leading to local phonon excitation around the remaining defect. Secondly, the iodine atom is not simply excited at its ground-state equilibrium position, but rather in form of a harmonic-oscillator wave function corresponding to its position-dependent ground-state potential. Consequently it will be expelled as a wave packet started by an initial Gaussian wave function. Thirdly, non-adiabatic dynamics has to be expected from coupling between the ground and excited states near 10 Å, which can not be described by classical mechanics but requires quantum mechanics of the nuclear motion instead [21].

5. Conclusions

Excited-state atom displacement and molecular dynamics within ab-initio approaches is still at its beginning. After successful development of excited state techniques like, e.g., many-body perturbation theory (GW method and Bethe–Salpeter equation), the interrelation with the geometry of the system is the natural next step.

Here we have compiled and compared several examples of systems that exhibit structural relaxation in the excited state, causing line broadening and Stokes shifts in the optical spectra. Such effects require localization of the excited state, which may either occur by external constraints or by self trapping. In some systems the geometry may not

simply relax to a new exited-state equilibrium, but may even dissociate when no total-energy minimum is found. Here we discussed the example of an alkali halide surface.

References

[1] G. Onida, L. Reining, A. Rubio, Rev. Mod. Phys. 74 (2002) 601.
[2] W.B. Fowler, in: W.B. Fowler (Ed.), Physics of Color Centers, Academic, New York, 1968.
[3] H. Koppel, W. Domcke, L.S. Cederbaum, Adv. Chem. Phys. 57 (1984) 59.
[4] E. Artacho, M. Rohlfing, M. Côté, P.D. Haynes, R.J. Needs, C. Molteni, Phys. Rev. Lett. 93 (2004) 116401.
[5] Y. Ma, M. Rohlfing, Phys. Rev. B 77 (2008) 115118.
[6] S. Ismail-Beigi, S.G. Louie, Phys. Rev. Lett. 90 (2003) 076401.
[7] J.C. Grossman, M. Rohlfing, L. Mitas, S.G. Louie, M.L. Cohen, Phys. Rev. Lett. 86 (2001) 472.
[8] H. Shi, R. Eglitis, G. Borstel, Phys. Rev. B 72 (2005) 045109.
[9] M.N. Kobrak, E.R. Bittner, J. Chem. Phys. 112 (2000) 5399.
[10] G. Grem, G. Leditzky, B. Ullrich, G. Leising, Adv. Mater. 4 (1992) 36.
[11] D. Hertel, S. Setayesh, H.-G. Nothofer, U. Scherf, K. Müllen, H. Bässler, Adv. Mater. 13 (2001) 65.
[12] P. Chiaradia, A. Cricenti, S. Selci, G. Chiarotti, Phys. Rev. Lett. 52 (1984) 1145.
[13] F. Ciccacci, S. Selci, G. Chiarotti, P. Chiaradia, Phys. Rev. Lett. 56 (1986) 2411.
[14] L. Reining, R. Del Sole, Phys. Rev. Lett. 67 (1991) 3816.
[15] J.E. Northrup, M.S. Hybertsen, S.G. Louie, Phys. Rev. Lett. 66 (1991) 500.
[16] M. Rohlfing, S.G. Louie, Phys. Rev. Lett. 83 (1999) 856.
[17] M. Rohlfing, J. Pollmann, Phys. Rev. Lett. 88 (2002) 176801.
[18] M. Szymonski, J. Kolodziej, Z. Postawa, P. Czuba, P. Piatkowski, Prog. Surf. Sci. 48 (1995) 83.
[19] A. Alexandrov, M. Piacentini, N. Zema, A.C. Felici, T.M. Orlando, Phys. Rev. Lett. 86 (2001) 536.
[20] W.P. Hess, A.G. Joly, K.M. Beck, M. Henyk, P.V. Sushko, A.L. Shluger, Surf. Sci. 564 (2004) 62.
[21] C. Carbogno, A. Groß, M. Rohlfing, Appl. Phys. A 88 (2007) 579.
[22] N.-P. Wang, M. Rohlfing, P. Krüger, J. Pollmann, Phys. Rev. B 67 (2003) 115111.